https://doi.org/10.21608/sjsci.2025.427800.1317

# Novel imine Complexes Incorporating Ca(II) and Mg(II) Cations: Synthesis and Antimicrobial Activity

#### Shimaa M. Abdel-Fatah\*

Chemistry Department, Faculty of Science, Sohag University, Sohag-82524, Egypt Corresponding author E-mail: shima mahdi@science.sohag.edu.eg

Received: 28th Septamber 2025 Revised: 18th Octaber 2025 Accepted: 22th Octaber 2025

**Published online:** 12<sup>th</sup> November 2025

**Abstract**: In this paper, Novel imine-complexes of Ca(II) and Mg(II) cations were synthesized and characterized. IR, TGA, UV/Vis, and 1HNMR techniques were used in conjunction with elemental (CHN), molar conductance and magnetic susceptibility experiments for characterization. None of the complexes are electrolytes, as shown by the conductivity measurements. All metal complexes exhibit diamagnetism, according to magnetic susceptibility data. Divalent cations favor a metal:ligand ratio of 1:1, depending on the analysis. Biological studies revealed that each compound had strong antimicrobial activity against a broad range of bacterial and fungal species. Furthermore, we observed that the antibacterial effectiveness of the M(II) complexes was arranged as follows: MgB > CaB > H<sub>2</sub>B. The Mg(II) combination was found to be the most effective against Gram-negative bacteria and to have the largest inhibition zone (25 mm). The following describes the antibiotic efficacy against the fungus *Aspergillus flavus*: MgB > CaB > H<sub>2</sub>B. According to this study, the produced substances have a high level of biological activity and may be useful in the fight against illnesses.

**Keywords:** Complexes, TGA, magnetic susceptibility, antimicrobial, bacteria.

#### 1. Introduction

Schiff bases play a significant part in living organisms, important type of ligands for coordination chemistry is the imine, which coordinates to metal ions via (azomethine nitrogen). Schiff bases are crucial for processes like (C-C) bond cleavage and transamination [1-4].

It is well known that the complexes have biological significance and serve as models for the structural analysis of metalloproteins and biomolecules. They can be used for a wide range of tasks in the fields of biology, medicine, analysis, and industry. A review of the literature shows that, in comparison to unchelated drugs, ligand/pure pharmaceuticals become more bacteriostatic upon complexation [5-7].

These days, a variety of approaches can be used to design and create molecular systems with biological and medicinal importance. Mycology has examined molecular systems with pyridine rings and chelating molecular designs in order to generate metal-based medications. Attempts have been made to make these medications using molecular devices based on pyridine. These metal-based medications' primary characteristics that contribute to their efficacy are their ability to penetrate the membranes of pathogenic cells and their affinity for the pathogens' genetic material (DNA or RNA) [8–11].

Calcium and magnesium Schiff base complexes are metal coordination compounds formed between calcium or magnesium ions and Schiff base ligands, which typically comprise nitrogen and oxygen donor atoms. These complexes have been investigated for various applications, including as catalysts for ring-opening polymerization of cyclic esters to

produce biodegradable polymers and in the development of sustained-release antibacterial agents. They are synthesized by reacting calcium or magnesium salts with Schiff base ligands in various solvents and can be characterized using various techniques [12-14].

Despite extensive research on metal complexes of Schiff bases, there is a lack of diverse metal ion exploration, comparative analyses, and detailed mechanistic insights. Therefore, in this work, we synthesize and thoroughly characterize a series of novel M(II) complexes, specifically Ca(II) and Mg(II) imine complexes, using a variety of analytical techniques. We evaluate these complexes' biological activities, focusing on their antimicrobial efficacy.

#### 2. Materials and methods

#### 2.1. Synthesis of imine ligand (H2B) and its M(II) complexes

#### 2.1.1. Imine ligand (H<sub>2</sub>B).

5-bromo salicylaldehyde (1.0 mmol, 0.201 g, 20 ml EtOH) was added to 2-amino-3-hydroxypyridine (1.0 mmol, 0.110 g, 20 ml EtOH). The reactants were blended for 45 min, followed by refluxing at 65 °C for 2 h, filtered and washed with ethyl alcohol (H<sub>2</sub>B); Yellow powder; yield, (71%); mp-225 °C; FTIR (cm<sup>-1</sup>): 3671 (-OH), 1620 (C=N), 1271 (C-O phenol). M.wt: 292.9 for C<sub>12</sub>H<sub>9</sub>O<sub>2</sub>N<sub>2</sub>Br UV/ vis ( $\lambda_{max}$ ): 266, 425, 516 nm. <sup>1</sup>H NMR ( $\delta$ , ppm): 7.25-8.08 (m, 6H-Ar), 9.48(s, 1H, CH=N), 10.22 (s, 1H, OH), 6.93 (s, 1H, OH); Elemental analysis: C 48.95; H 3.22; N 9.56 (Calculated: C, 49.16; H, 3.07; N, 9.55).

#### 2.1.2. Ca(II) complex{CaB}.

Ligand ( $H_2B$ ) (1 mmol, 0.292 g, 30 ml EtOH) was added up to  $Ca(NO_3)_2 \cdot 4H_2O$  (1.0 mmol, 0.236 g, 30 ml EtOH). The

reaction mix were refluxed in ethanol at 65 °C for 3 h, filtered and washed with ethanol; orange powder; yield, (81 %); mp-(>300) °C; FTIR (cm<sup>-1</sup>): 3233 (H<sub>2</sub>O<sub>hydr</sub>), 1630(C=N), 1273(C-O phenol), 890 (H<sub>2</sub>O<sub>coord</sub>), 524 (M-O), 465 (M-N). UV/ vis ( $\lambda_{max}$ ): 305, 462, 533, 683 nm. M.wt: 384.98 for C<sub>12</sub>H<sub>13</sub>O<sub>5</sub>N<sub>2</sub>BrCa; Elemental analysis: C 37.51; H 3.25; N 7.31 (Calculated: C, 37.40; H, 3.37; N, 7.27). Λm ( $\Omega^{-1}$ cm<sup>2</sup>mol<sup>-1</sup>): 4.76;  $\mu_{eff}$  (B.M): diamagnetic.

#### 2.1.3. Mg(II) complex{MgB}.

Ligand (H<sub>2</sub>B) (1 mmol, 0.292 g, 30 ml EtOH) was added up to Mg(NO<sub>3</sub>)<sub>2</sub>·6H<sub>2</sub>O (1.0 mmol, 0.256 g, 30 ml EtOH). The reaction mix were refluxed in ethanol at 60 °C for 3-4 h, filterated and rinsed with ethanol; orange powder; yield, (76 %); mp-(>300) °C; FTIR (cm<sup>-1</sup>): 3205 (H<sub>2</sub>O<sub>hydr</sub>), 1625(C=N), 1265(C-O phenol), 880 (H<sub>2</sub>O<sub>coord</sub>), 515 (M-O), 438 (M-N). UV/vis ( $\lambda_{max}$ ): 311, 455, 531, 675 nm. M.wt: 369.20 for C<sub>12</sub>H<sub>13</sub>O<sub>5</sub>N<sub>2</sub>BrMg; Elemental analysis: C 39.05; H 3.45; N 7.62 (Calculated: C, 39.00; H, 3.52; N, 7.58). Am ( $\Omega^{-1}$ cm<sup>2</sup>mol<sup>-1</sup>): 6.89; μ<sub>eff</sub> (B.M): diamagnetic, Scheme 1.

**Scheme 1.** Structure of complexes with divalent cations (M(II) = Ca and Mg).

### 2.2. Physical characterization

#### 2.2.1. Equipments

The melting point was determined via Gallenkamp apparatus, UK; Shimadzu FTIR spectrophotometer was used to capture their IR spectra (model 8101); whereas DMF was used as solvent to assess their UV-visible (Uv-Vis) spectra using PG spectrophotometer; model T+80. DMSO-d6 and a Bruker apparatus running at 400 MHz were employed to produce <sup>1</sup>H and <sup>13</sup>C NMR spectra, with TMS acting as an internal standard. In DMF, conductivity was measured utilizing a Jenway conductivity meter (model 4320). A Shimadzu Corporation 60H analyzer running in N2 with a heat rate of {10 °C min-1}

was applied to conduct a thermogravimetric test.

Perkin-Elmer Elemental analyzer (model 240c) at Cairo University was employed for elemental analysis; Measure of the magnetic property was made using Gouy's balance. A HANNA 211 pH meter had been employed to measure the pH at 298 K. At various pH levels, the absorbance values of  $1 \times 10^{-3}$  M of each complex were recorded. Several Britton universal buffers were employed to assess the pH levels.

#### 2.2.2. Chemicals

Sigma-Aldrich Chemie (Germany) provided all of the chemicals utilized during this investigation, comprising 5-bromosalicylaldehyde, 2-amino-3-hydroxypyridine, and metal salts such  $Ca(NO_3)_2 \cdot 4H_2O$  and  $Mg(NO_3)_2 \cdot 6H_2O$ . Dimethylsulfoxide (DMSO), dimethylformamide (DMF), and ethanol of spectroscopic grade were employed.

#### 2.3. Antimicrobial potency

The paper disc method was implemented to evaluate the imine ligand and its metal complexes' antifungal and antibacterial effects (*Escherichia coli, Micrococcus luteus, Aspergillus flavus*) at a concentration of 20  $\mu$ g/ml in DMSO [15–19]. Both fluconazole and ofloxacin were employed as antifungal and antibacterial agents, respectively.

#### 3. Results and Discussion:

#### 3.1. Physicochemical properties

The most common organic solvent in which all M (II) complexes dissolve is DMSO. Divalent cations favor a metal:ligand ratio of 1:1, based on the analysis. <sup>1</sup>H NMR spectra refer to formation Schiff base. The geometry of complexes is octahedral based on various techniqes. The diamagnetism of every M(II) complex is supported by magnetic susceptibility data. The theoretical spin-only magnetic values for calcium and magnesium complexes are zero, meaning there are no unpaired electrons. Magnetic susceptibility measurements for the prepared imine complexes were calculated according to the following:

$$\mu_{eff} = 2.83 \sqrt{\chi'_{M}T}$$
 $\chi'_{M} = \chi_{M} - (diamag.corr.)$ 

Where T is the temperature (K),  $\mu$ eff is the magnetic moment in Bohr Magneton (BM) and  $\chi$ M is the molar magnetic susceptibility before correction, and  $\chi$ 'M is the molar magnetic susceptibility after correction [20-22]..

#### 3.1.1. Infrared spectroscopy

In the IR spectra obtained for the (H<sub>2</sub>B) ligand, the azomethine group is responsible for the ligand's sharp band at 1620 cm<sup>-1</sup>. The spectrum also includes characteristic IR band at 1271 cm<sup>-1</sup>, consistent with the existence of phenolic {C–O} group, The complexation with the azomethine (H-C=N) group is expected to result in an intense band in the extent of 1625–1630 cm<sup>-1</sup> in all of the M(II) complexes; that confirm complexation between ligand and metal ions. The spectra also include characteristic IR bands at 1265-1273 cm<sup>-1</sup>, consistent with the existence of phenolic {C–O} group, It's significant that all the M (II) complexes exhibit comparatively prominent IR bands between 880 and 890 cm<sup>-1</sup>, which are explained by

the existence of coordinated water molecules. The IR bands detected at 438-465 and 515-554 cm<sup>-1</sup>, which can be assigned to both {M-N} and {M-O} stretching vibrations, respectively, were utilized to determine the presence of metal ions in these complexes, as shown in Figure (1, S1) [23-24].

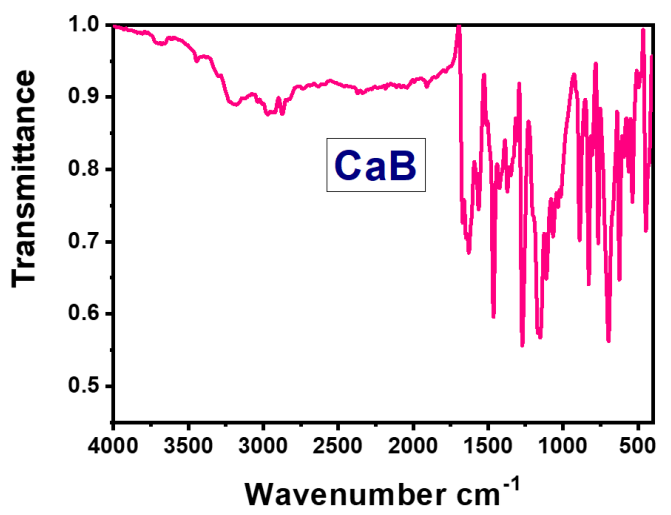


Fig 1: FT-IR spectra of CaB complex.

#### 3.1.2. <sup>1</sup>HNMR and <sup>13</sup>CNMR of the prepared imine ligand

The <sup>1</sup>H-NMR spectra of the imine ligand show signals at  $(7.25-8.08; (m) \delta)$ , for aromatic protons and  $(9.48; (s) \delta)$ , for proton of the azomethine; that confirm the formation of imine. The peaks at  $(10.22 \text{ (s)}, 6.93 \text{ (s)} \delta)$  resulted from –OH groups [25-26]. The <sup>13</sup>C-NMR spectra of the imine ligand show signals at (160.26 ppm), for azomethine carbon, (111.16-150.44 ppm) for aromatic carbons, as shown in Figure S2, S3.

#### 3.1.3. Electronic spectra

Electronic spectra of ( $H_2B$ ) ligand displays an absorption band at ~266 nm, which is attributed to the  $\pi$ - $\pi$ \* transition, and an absorption band at ~425 nm, that is assigned to the n- $\pi$ \* transition. Metal complexes show absorption band at 455-533 nm, which approves the transfer of electrons from the ligand to the metal (LMCT) which is caused by the complexation of the nitrogen atom to the metal ions. The significant changes in optical density for complexes in comparison to the ligand support the coordination between ( $H_2B$ ) ligand and M(II) ions in the prepared complexes, as shown in Figure 2 [27].

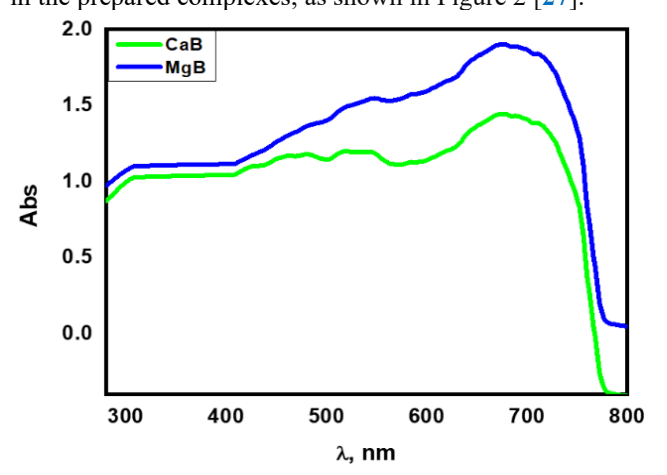


Fig 2: Electronic spectra of the prepared imine-M(II) complexes.

#### 3.1.4. Thermal Analysis

Thermal test was implemented under N<sub>2</sub> with a rate of heating 10 °C min<sup>-1</sup>. The thermal degradation happened in three stages (removal of water molecules of hydration then coordinated water molecules and finally removal of organic moiety). The CaB and MgB possess weight wastages of 4.54 and 9.68 % respectively, that are resulted from loss of hydrated water molecules. The weight wastages of (9.42, 20.08, 51.53 %) coinciding to the loss of the residual fraction of the complex at {140-999 °C} for CaB complex. The weight wastages of (4.95, 53.69, 20.68 %) coinciding to the loss of the residual fraction of the complex at {147-999 °C} for MgB complex, Table S1 and Figure S4[3]. The end product manifested from a horizontal curve has been gained proposing forming of metal oxide (CaO, MgO), Scheme 2. The metal complexes have high thermal stability.

$$\begin{bmatrix} \mathsf{Br} & \mathsf{N} \\ \mathsf{O} & \mathsf{Ng} & \mathsf{O} \\ \mathsf{OH}_2 & \mathsf{OH}_2 \end{bmatrix} \cdot \mathsf{H}_2\mathsf{O}_{-2\mathsf{H}_2\mathsf{O}} \cdot \mathsf{Br} \qquad \mathsf{Br} \quad \mathsf{O}_{-\mathsf{Mg}} \quad \mathsf{O$$

**Scheme2:** TGA for the prepared MgB complex under N<sub>2</sub> with a rate of heating 10 °C min<sup>-1</sup>.

## 3.1.5. Kinetic aspects for TGA of the prepared imine complexes

The Coats-Redfern equation was applied for estimating the thermodynamic parameters of the complexes' decaying process. As can be seen in Table S2, the complexes were more ordered than the reactant and the reactions were slower when the activation entropy had a negative number. H\* and G\*, which stand for endothermic characteristics for all stages, were shown to have values that are positive.

shown to have values that are positive.
$$\log \left[ \frac{\log w_{\infty} / (w_{\infty} - w))}{T^2} \right] = \log \left[ \frac{AR}{\phi E^*} \left( 1 - \frac{2RT}{E^*} \right) \right] - \frac{E^*}{2.303RT}$$

Where  $W\infty$  is the mass loss at the completion of the decomposition reaction. W is the mass loss up to temperature

T, R is the gas constant and  $\Phi$  is the heating rate. Since 1-2RT/E\*  $\approx$ 1, the plot of the left-hand side of equation against 1/T would give a straight line. E\* was then calculated form the slope and the Arrhenius constant, A, was obtained from the intercept. The other kinetic parameters; the entropy of activation (S\*), enthalpy of activation (H\*) and the free energy change of activation (G\*) were calculated using the following equations:

$$S^* = 2.303R \log \frac{Ah}{k_B T}$$
  
 $H^* = E^* - RT$ ,  $G^* = H^* - TS^*$ 

Where  $(k_B)$  and (h) are Boltzmann's and Plank's constants, respectively [9].

Research Article SOHAG JOURNAL OF SCIENCES

## 3.1.8. Electronic absorption spectra of the prepared imine complexes at different pH values

The absorbance vs. pH (pH-profile) depicted in Figure (3) displayed a high stability pH range along with typical dissociation curves. This indicates that the imine ligand is significantly stabilized upon complex formation. Thus, the pH range of pH = 4 to pH = 10 is appropriate for the different fields of the complexes that have been studied.

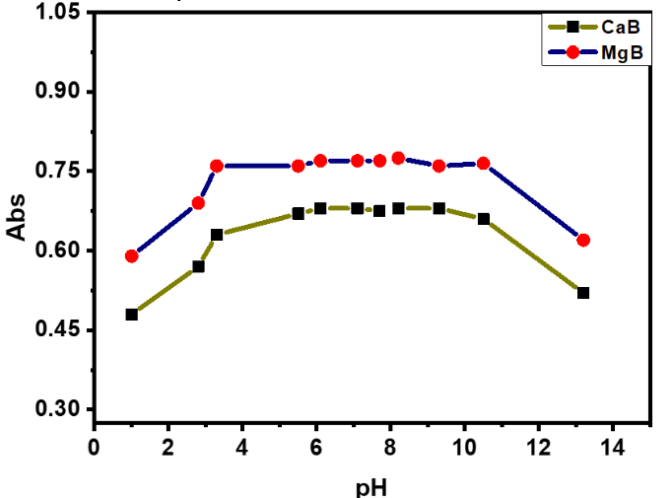


**Fig 3:** Dissociation curves of the prepared imine complexes in aqueous ethanol mixture at [complex] =  $1 \times 10^{-3}$  mol L<sup>-1</sup> and 298 K.

#### 3.2. Antimicrobial activity

The inhibition zone (mm); which is presented in Table S3, was measured in order to assess the antimicrobial potency. The standards used for the antibacterial and antifungal tests were ofloxacin and fluconazol, respectively.

Additionally, we found that the M(II) complexes' antibacterial potency was on the order of ofloxacin > MgB > CaB > H2B. It was found that the MgB combination was the most effective versus Gram-negative bacteria and had the largest inhibition zone (25 mm). Chelation theory and the Overtone's concept were used to illustrate this phenomenon. The donor atoms in the ligand share some of the positive charge of the M(II) ion in a complex, causing electron delocalization throughout the entire chelated ring. As a result, the bacterial membrane's lipoid layers increased.

The remaining compounds' antimicrobial efficacy against fungus in descending order (*Aspergillus Flavus*): fluconazol > MgB > CaB > H<sub>2</sub>B which are presented in Figure 4. This research demonstrated that the prepared compounds have high biological activity and could effectively combat diseases. The results of this research are superior to those of previous studies [28-32].

The Mg(II) complex had the maximum activity index (96.15%) and was the most efficient against *Escherichia coli*, as displayed in Table S4. Additionally, the Mg(II) complex had the maximum activity index (91.66%) and was the most efficient against *Aspergillus flavus*.

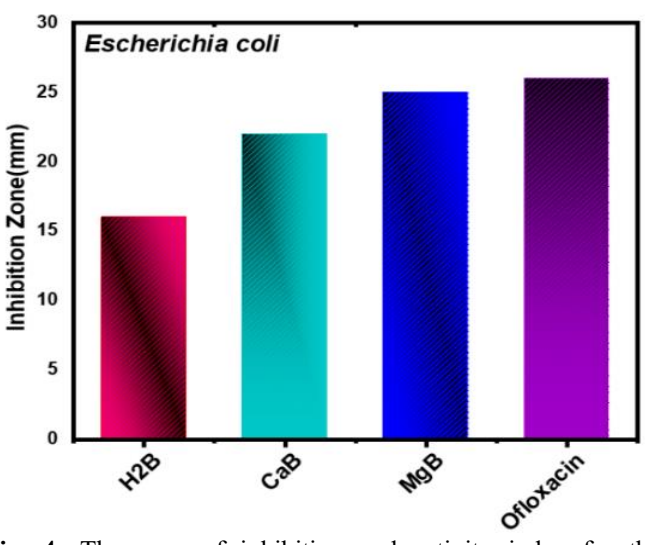


**Fig. 4:** The zone of inhibition and activity index for the prepared (H<sub>2</sub>B) and its M(II) complexes against (*Escherichia coli*).

#### 4. Conclusion

A variety of analytical techniques were employed in this work to produce and analyze Schiff base (H2B) and its (Ca(II) and Mg(II)) imine complexes. The structure and composition were confirmed through the use of NMR spectroscopy, FTIR, and elemental analysis. Every metal (II) complex exhibits diamagnetism properties, according to magnetic susceptibility data. Divalent cations favor a metal:ligand ratio of 1:1, depending on the analysis. Furthermore, all M(II) complexes demonstrate exceptional inhibitory activity against the strains of bacteria and fungi that were investigated compared to free ligand. The findings from this research suggest that the synthesized metal-imine complexes possess therapeutic properties. Using novel metal-based drugs as anticancer and anti-inflammatory agents was recommended.

#### Data availability statement

The data used to support the findings of this study are available from the corresponding author upon request.

#### References

- [1] S. M. Abdel-Fatah, M. T. Basha, B. S. Al-Farhan, M. R. Shehata, and L. H. Abdel Rahman, *Appl. Organomet. Chem.* 39 (2025) 7785.
- [2] L. H. Abdel-Rahman, B. S. Al-Farhan, N. O. Al Zamil, M. A. Noamaan, H. E. Ahmed, and M. S. S. Adam, *Bioorg. Chem.* 114 (2021) 105106.
- [3] L.H. Abdel-Rahman, R.M. El-Khatib, S.M. Abdel-Fatah, H. Moustafa, A.M. Alsalme, and A, Nafady, *Appl. Organomet. Chem.* 33 (2019) 5177.
- [4] S.M. Abdel-Fatah, M. Díaz-Sánchez, D. Díaz-García, S. Prashar, S. Gómez-Ruiz, L.H. Abdel-Rahman, J. Inorg. Organomet. Polym. 30 (2020) 1293.
- [5] L.H. Abdel-Rahman, R.M. El-Khatib, A.M. Abu-Dief, S.M. Abdel-Fatah and A.A. Sleem, *Int. J. Nano. Chem.* 2 (2016) 83
- [6] L.H. Abdel-Rahman, A.M. Abu-Dief, R.M. El-Khatib, and

#### **Research Article**

- S.M. Abdel-Fatah, *Bioorg. Chem.* 69 (2016) 140.
- [7] L.H. Abdel-Rahman, R.M. El-Khatib, A.M. Abu-Dief, and S.M. Abdel-Fatah, J. Photochem. Photobio B. 162 (2016) 298.
- [8] S.I. Al-Saeedi, L.H. Abdel-Rahman, A.M. Abu-Dief, S.M. Abdel-Fatah, T.M. Alotaibi, A.M. Alsalme and A. Nafady, *Catalysts*, 8 (2018)452.
- [9] S. M. Abdel-Fatah, L. H. Abdel Rahman, M. R. Shehata, *sohag J. Sci.* 10 (2025) 124.
- [10] S. M. Abdel-Fatah, M. T. Basha, A. I. Al-Sulami, M. R. Shehata and L. H. Abdel Rahman, Appl. Organomet. Chem. 39 (2025) 70192.
- [11] L. H. Abdel-Rahman, S. F. Alzarzah, M. Abdel-Hameed, M. R. Shehata, A. El-Saghier, Appl. Organomet. Chem. 38(2024)7631.
- [12] L. H. Abdel-Rahman, M. S.S. Adam, N. Al-Zaqri, M. R. Shehata, H. E. Ahmed, S. K. Mohamed, *Arab. J. Chem.* 15 (2022)103737..
- [13] L.H. Abdel-Rahman, M.T. Basha, B.S. Al-Farhan, M.R. Shehata, E.M. Abdalla, *Appl. Organomet. Chem.* 36 (2022) 6484.
- [14] L. H. Abdel-Rahman, R. M. El-Khatib, L. A. E. Nassr, A. M. Abu-Dief, M. Ismael, A.A Seleem, Spectrochim. Acta Part A: Mol. Biomol. Spectro. 117 (2014) 366.
- [15] NCCLS., Methods for Anti-Microbial Dilution and Disk Susceptibility Testing of Infrequently Isolated or Fastidious Bacteria; Approved Guideline Document M45-A. National Committee for Clinical Laboratory Standrd., Villanova PA USA, 26(1999).
- [16] N.P. Priya, S.V. Arunachalam, N. Sathya, V. Chinnusamy, C. Jayabalakrishnan, Transition Met. Chem. 34 (2009) 437.
- [17] A.A.A. Emara, Spectrochim. Acta, Part A, 77 (2010) 117.
- [18] S. Jain, R. Sharma, V. Jain, R.C. Jat, S. Dubey, S. Bhardwaj, J. Pharm. Res. 3 (2010) 274.
- [19] A.W. Bauer, W.M.M. Kirby, J.C. Sherris, M. Turck, Am. J. Clin. Pathol. 45 (1966) 493.
- [20] W.J. Geary, Coord. Chem. Rev. 7 (1971) 81.
- [21] P.K. Radhakrishnan, Inorg. Chim. Acta, 110 (1985) 211.
- [22] W. Plass, G. Fries, Z. Anorg. Allg. Chem. 623 (1997) 1205.
- [23] K. Mohanan, S.N. Devi, Russ. J. Coord. Chem. 32 (2006) 600.
- [24] K. Mohanan, C.J. Athira, Y. Sindhu, M.S. Sujamol, J. Rare Earths. 27 (2009) 705.
- [25] K. Kumar, S. Murugesan, T. Muneeswaran, C. Ramakritinan, Cur. Chem. Lett. 12 (2023) 721.
- [26] A. Cinarli, D. Gurbuz, A. Tavman, A.S. Birteksz, Bull. Chem. Soc. Ethiop. 25 (2011) 407.
- [27] A. Matwijczuk, D. Karcz, R. Walkowiak, J. Furso, B. Gładyszewska, S. Wybraniec, A. Niewiadomy, G.P. Karwasz, M. Gagos', J. Phys. Chem. A, 121 (2017) 1402.
- [28] M.T. Kaczmarek, M. Zabiszak, M. Nowak, R. Jastrzab, Coord. Chem. Rev. 370 (2018) 42.
- [29] Y. Anjaneyula, R.P. Rao, Synth. React Inorg. Met-Org. Chem. 16 (1986) 257.
- [30] B.G. Tweedy, *Phytopathology*, 55 (1964) 910.
- [31] A. M. Abu-Dief, T. El-Dabea, R. M. El-Khatib, A. Abdou, I. O. Barnawi, H. A. Alshehri and M. A. E. A. Ali, *J. Mol. Struc*. 1310 (2024)138328.
- [32] A. M. Abu-Dief, T. El-Dabea, R. M. El-Khatib, M. Feizi-Dehnayebi, F. S. Aljohani, K. Al-Ghamdi and M. A. E. A. A. Ali, J. Mol. Liq. 399(2024) 124422.